한국해양공학회지 제20권 제3호, pp 7~14, 2006년 6월 (ISSN 1225-0767)

A Study on the Structural Design and Analysis of a Deep-sea Unmanned Underwater Vehicle

TAE-HWAN JOUNG*, JAE-HWAN LEE**, IN-SIK NHO**, JONG-MOO LEE*** AND PAN-MOOK LEE***

*School of Informatics and Engineering, Flinders University, Adelaide, Australia
**Dept. of Naval Architecture and Ocean Engineering, Chungnam University, Daejeon, Korea
***Maritime and Ocean Engineering Research Institute, KORDI, Daejeon, Korea

KEY WORDS: ROV (Remotely operated vehicle) Launcher, Structural analysis, Finete element analysis, Optimum design, Buckling analysis

ABSTRACT: *This paper discusses the structural design and analysis of a 6,000 meters depth-rated capable deep-sea unmanned underwater vehicle (UUV) system. The UUV system is currently under development by Maritime and Ocean Engimeeimg Rereauch Institute(MOERI), Korea Ocean Research and Development Institute (KORDI). The UUV system is composed of three vehicles - a Remotely Operated Vehicle (ROV), an Autonomous Underwater Vehicle (AUV) and a Launcher - which include underwater equipment. The dry weight of the system exceeds 3 tons hence it is necessary to carry out the optimal design of structural system to ensure the minimum weight and sufficient space within the frame for the convenient use of the embedded equipments. In this paper, therefore, the structural design and analysis of the ROV and launcher frame system were carried out, using the optimizing process. The cylindrical pressure vessels for the ROV were designed to resist the extreme pressure of 600 bars, based on the finite element analysis. The collapse pressure for the cylindrical pressure vessels was also checked through a theoretical analysis.*

1. Introduction

In the past, ROV (Remotely operated vehicles) started to be developed in order to accomplish minor roles in places where diver's work was impossible or just for general scientific research. Recently, however, such vehicles have various uses in the development of deep-sea resources, the installation or repair of communication lines or rescue work, etc.

An ROV is composed of a frame, buoyant material, control and navigation devices, manipulators and pressure vessels which are able to protect the various electronic devices. Among the structural elements of ROVs, especially, the frame and the pressure vessels must have thorough safety investigation through structural analysis before construction, because the structural safety of ROV is affected by the weight of the electronic devices, their location, their size, static or kinetic loads and deep-sea pressure.

In this paper, firstly, the structural design and analysis of the launcher and ROV frame that will be used in 6,000m deep-sea have been conducted. The authors tried to distribute the weights of the various devices and buoyant material, and then performed the linear-elastic analysis with ANSYS for the initial design plan. After the sensitivity analysis, optimum frame design was carried out.

교신저자 정태환: Flinders University, Adelaide, Australia
+61-8-8201-3614 taehwan.joung@flinders.edu.au

Secondly, in the deep-sea, very high water pressure is acting on the ROV, while the pressure vessels have to maintain atmospheric pressure on the inside. Therefore, it was investigated that the pressure vessels are able to withstand the extremely high pressure which is equivalent to that at the depth of 6,000m (600bar) from the sea surface. Two cylindrical pressure vessels have been designed. One had no stiffener and the other was ring stiffened one. The two pressure vessels have had safety checks through the linear-elastic analysis by FEM, elasto-plastic analysis and buckling analysis by theoretical formulae.

2. Structural Design and Analysis of the Launcher and ROV's Frames

The 3-D conceptual models of launcher and ROV are shown in Fig. 1. The launcher frames will be made of galvanized steel and ROV frames will be made of aluminum 60 series (AL6061-T6).

The launcher is considered as an underwater base for the operation of ROV. So it has to play a very important role in the working system to reduce the impact loads due to the wave induced motion of the mother ship. On the other hand the ROV was designed for easy operation in the water by use of aluminum 60 series (AL6061-T6), which has light and corrosion-resistance characteristics. And the launcher has been

Table 1 Material properties of UUV frame

Material	Density [g/cm^3]	Elastic modulus [GPa]	Possion's ratio	Yield strength [MPa]	Tensile strength [MPa]
Galvanized steel	7.85	210	0.29	250	350
Al6061-T6	2.7	70	0.33	270	310

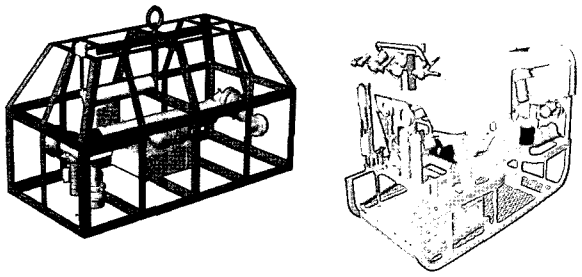

Fig. 1 Concept design of the launcher and ROV

designed to use galvanized steel with an appropriately selected gravity (Nho and Joung, 2003).

2.1 Structural design and analysis

The sections of the members of frames which will be used for the launcher and ROV are 4 and 7 types, respectively. The element which has been used for the finite element analysis (FEA) is the beam element (BEAM188) which is a 3-D graphic element that can simulate structural behaviors of frame realistically.

Boundary and load conditions have to be taken into consideration when the ROV system is lifted in the air. The structural safety of frames are judged based on the yield stresses of materials, considering safety factors for live load, strength loss due to welding and load caused by unexpected impact. In this study, it has been decided that the minimum safety factor of 8 is needed for the safety of the system (Lee and Joung, 2004).

The FEA result (von-Mises equivalent stress) for the launcher which has initially designed sections is shown in Fig. 2. The maximum displacement is about 0.58mm, which is slight, and it occurred in the central frame of the base. The maximum stress is about 14.7MPa and it occurred in the same position. These are considered to be due to the load of controller box and pressure vessels which are concentrated in the base of the frame structure. The safety factor is above 8 and it seems to be safe enough for material yielding, even if the live load, strength loss due to welding and load caused by unexpected impact would be considered. Therefore, the

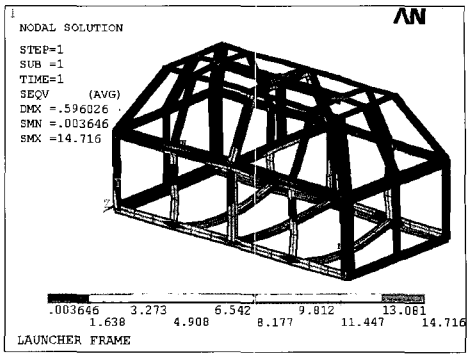

Fig. 2 Stress result of the launcher (initial design)

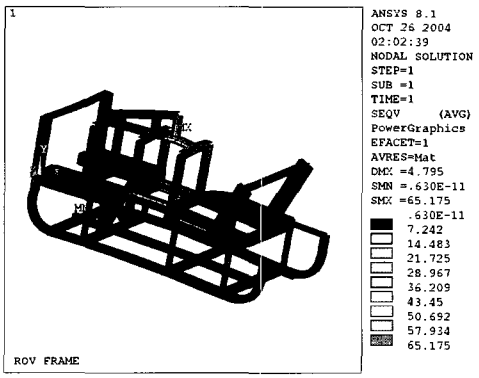

Fig. 3 Stress result of the ROV frame (initial design)

weight of the launcher could be reduced by optimum design process.

On the other hand, the FEA result (von-Mises equivalent stress) for the ROV which has initially designed sections is shown in Fig. 3. The maximum displacement is about 4.8mm and it occurs in the stem. This is thought to be caused by two manipulators that are installed in the stem. Moreover, the place in which manipulators will be set up may incur a lot of stress partially due to the work conditions in the deep-sea.

The maximum stress of the ROV frame is about 65MPa as shown in Fig. 3. The calculated safety factor for yield stress (270MPa) of Al6061-T6 is about 4, and is less than that of previous launcher frame of 8. Therefore the authors tried to raise the safety factor up to 8, while reducing the weight through optimum design process.

2.2 Optimum design and sensitivity analysis

The optimum designs to minimize the weight of frame structures were carried out, satisfying the regular responses (displacement and stress) criteria, for a given load and constraints. In the formularization for the optimum design, various design variables such as the thicknesses, the heights and the widths for the sections are used. Displacement was

used as a constraint function, and to get the minimum weight, the total weight of the frame was selected as object function.

Optimization of the frame sections was carried out by ANSYS, using the Sub-program method and the First-program method. The Sub-program method is a global searching method to avoid a local optimum point by using an approximate value. The execution time to find the optimum point is very fast, but the accuracy is unreliable. On the other hand, however, the First-program method uses the differential of object function and constraints, instead of an approximate value, so it can give quite accurate results. Therefore, in this study, firstly, the result that had been computed by the Sub-program method was fixed as an initial point, and then the optimum point was searched by executing the First-program method. At the derived optimum points, the sensitivity values of each design variables have been calculated.

In table 2, SET 1 is the FEA results of the initial design, SET 2 is the FEA results of the optimum point on the ANSYS, and SET 3 is the FEA results after the authors going through the whole process of optimum design of the launcher and ROV frame.

In the case of the launcher, after going through the whole process of optimum design by the authors (SET3), the weight of approximately 116kg$_f$ (42%) has been decreased. The displacement and the stress have increased a little from 0.583mm and 14.72MPa to 1.2mm and 28.3MPa, respectively. This level is, however, considered to be sufficiently safe, because the safety factor is 8.62 compared with the previous safety factor of 8.

On the other hand, after the optimum design process, the ROV reduced its weight by 87kg$_f$ (26%). The maximum value

Table 2 Comparison of initial design, optimum design and redesign

Frame	Results	SET1	SET2	SET3
Launcher Frame	Displacement [mm]	-0.583	-1.05	-1.163
	von-Mises stress [MPa]	14.72	28.45	28.30
	Weight [kgf]	276.63	160.55	160.21
ROV Frame	Displacement [mm]	-4.56	-5.04	-5.06
	von-Mises stress [MPa]	66.44	62.44	61.31
	Weight [kgf]	331.56	245.32	244.59

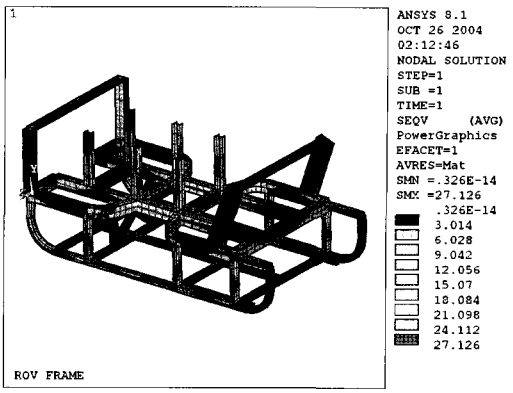

Fig. 4 Stress result of the ROV frame (optimum design)

of von-Mises equivalent stress of the ROV frame is 61MPa. The safety factor for yield stress of AL6061-T6 is 4.5, which is insufficient for the criterion of design safety factor. As shown in Fig. 4, however, except the joint for lifting the overall stress level is less than 27MPa which is under the safety factor of 8. Consequently, this ROV is a safe structure and the target safety factor can be satisfied by reinforcing the joint for lifting.

3. Structural Design of the Pressure Vessel

3.1 The design conditions

Generally, Ti alloy (Ti-6Al-4V) and Al alloy (Al7075-T6) could be considered as materials suitable for the pressure vessels of UUV. In this case, the chosen material is AL7075-T6. To analyze the pressure vessels, the material properties of AL7075-T6 such as elastic modulus, Poisson's ratio, yielding stress and ultimate stress are used as 72GPa, 0.33, 480MPa and 550MPa, respectively.

The length, the diameter and the thickness of the pressure vessel could be determined according to the size of the electronic devices that would be installed inside. Thus, the design dimensions which depend on the sizes of the electronic devices could be changeable, and the pressure vessel design should be adaptable, depending on the required working pressure.

3.2 Tangent modulus

For the plastic buckling analysis, tangent modulus (E_t) is needed in a plastic region. Since AL7075-T6 does not have a clearly observable yielding phenomenon such as steel (O-shima, 1972), the Ramberg-Osgood curve was used in this study. The Ramberg-Osgood curve is known to be suitable for materials which do not show a yielding phenomenon. Tangent modulus (E_t) can be expressed by using parameters

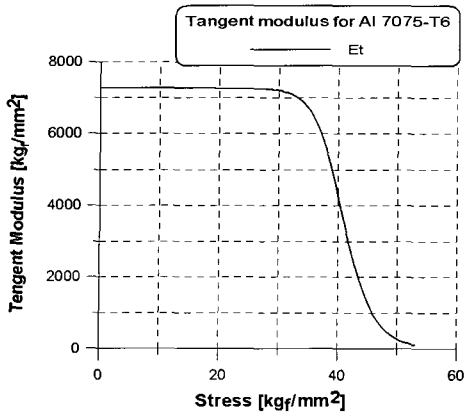

Fig. 5 Tangent modulus for Al7075-T6

such as u, w and σ_1 as follows:

$$E_t = \frac{E}{1 + \frac{u(1-\omega)}{\omega}\left(\frac{\sigma}{\sigma_1}\right)^{u-1}} \quad (1)$$

Where u, w and σ_1 can be determined by material tests. Especially, σ_1 is a parameter which was obtained by the processing of expression from the real test curve to the Ramberg-Osgood curve is 38.4kg$_f$/cm^2. By using the parameters, tangent modulus (E_t) can be determined by the formula (2). A graph of the Tangent modulus (E_t) is shown in Fig. 5 (Shin and Woo, 1999).

$$E_t = \frac{7258.77}{1 + \frac{17(1-0.979)}{0.979}\left(\frac{\sigma}{38.4}\right)^{u-1}} \quad (2)$$

3.3 The design of the pressure vessels

3.3.1 The unstiffened cylinder

It is more effective for the structure to resist high pressure as a membrane form rather than as a form that resists bending. Thus, the pressure vessels should be shaped such as a sphere, generally. However, in order to arrange the electronic devices efficiently, the cylinder as in Fig. 6 is used and for the covering, a hemisphere or an endplate are used (Ura and Takagawa, 1997).

Initial scantlings of the unstiffened cylindrical pressure vessel such as the length (L), the inside diameter (D_i) and the thickness (t) are 600mm, 250mm and 25mm respectively. For the linear-elastic analysis of this cylinder, Finite Element Analysis (FEA) and a theoretical formula that was suggested by Warren C. Young were used (Young, 1989). The safety check of the buckling analysis has been verified via buckling pressure formulae of Shin and Woo (Shin and Woo, 1999).

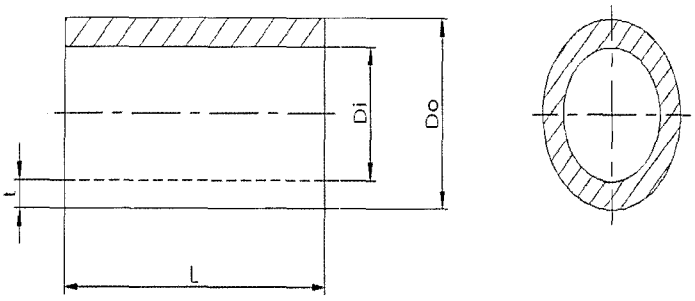

Fig. 6 Dimensions of a unstiffened cylinder

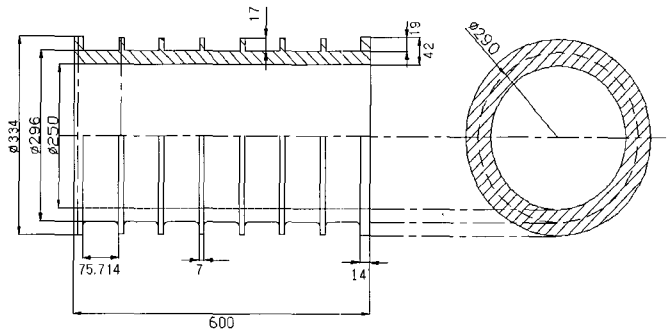

Fig. 7 Dimensions of the unstiffened cylinder

3.3.2 The stiffened cylinder

A pressure vessel that is reinforced with ring-type stiffeners has excellent efficiency to withstand high pressure, compared with one that is not. The stiffened cylinder enables the pressure vessel withstand higher buckling pressure. Especially, general buckling can be prevented.

The cylindrical part of the pressure vessel which has been reinforced with a ring stiffener as shown in Fig. 7 was designed. The weight is about 32kg, which means it weighs about 4kg lighter than the previously shown cylinder without reinforcement. The safety of the cylinder has been verified as following procedures for linear-elastic analysis, Finite Element Analysis has been used, and for buckling analysis, the general buckling pressure and the partial buckling pressure have been verified by ABS formulae (ABS, 1990).

4. Structural Analysis of The Pressure Vessel

4.1 Linear-elastic analysis

4.1.1 The unstiffened cylinder

The shape of the pressure vessel and the applied load and boundary conditions are axi-symmetric. So the pressure vessel can be analyzed by an axi-symmetric element with a two-dimensional section (Deepsea Power&Light, 2001). The used element is 2-D 8-node structural solid (PLANE82), and

the number of elements is 30 the number of nodes is 125. The load of 600bar has been applied to the external wall, and atmospheric pressure has been applied to the inner wall. For the boundary condition, a symmetric condition was applied (ANSYS, 1994).

As a result of the linear-elastic analysis using Finite Element Analysis software (ANSYS 8.01), the maximum displacement is 0.63mm and the circumference direction stress (hoop stress) and von-Mises equivalent stress are 392MPa and 339MPa respectively, which occur at the inner wall as depicted in Fig. 8.

The results of Warren C. Young's theory show that the maximum displacement is 0.67mm, the hoop stress is 393MPa and von-Mises equivalent stress is 340MPa. Thus, the FEA result and analytical results agree with each other very closely. The cylinder part seems to be safe until the maximum depth of 8,279m.

4.1.2 The stiffened cylinder

The load condition and the element used are same as the case of unstiffened cylinder. The number of elements is 281 and the number of nodes is 1068. The boundary condition, however, is slightly different from the case of the unsifffened cylinder. To avoid occurring stress concentration, both ends are coupled (ANSYS, 1994; JAMSTEC, 1991).

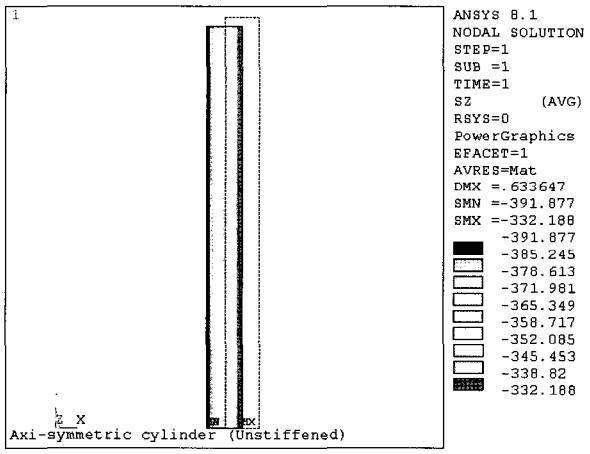

Fig. 8 Hoop stress contours of unstiffened cylinder

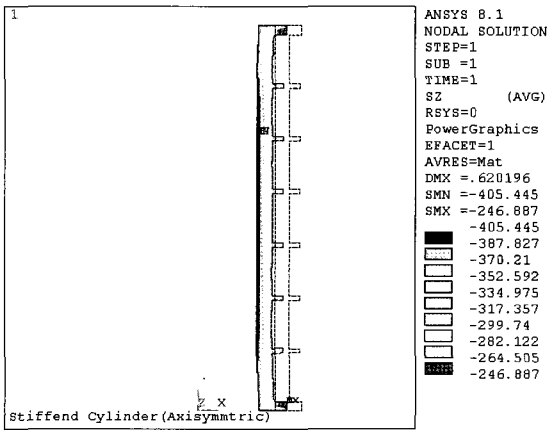

Fig. 9 Hoop stress contours of stiffened cylinder

As a result of the linear-elastic analysis, the maximum stress is a hoop stress of about 405MPa, which occurred in the inner wall, as shown in Fig. 9. Compared with the result of unstiffened cylinder, the maximum stress increased about 15MPa, but the general stress level decreased by 20~80MPa. Only considering linear-elastic analysis, the cylinder seems to be safe until the maximum depth of 7,100m.

4.2 The buckling analysis

4.2.1 The unstiffened cylinder

In order to check the buckling strength, the formula which was suggested by Shin and Woo for the unstiffened cylinder was used (Shin and Woo, 1999). The buckling stress and pressure for the unstiffened cylinder are described in formulae (3) and (4).

$$G=\frac{\sigma_{cr}}{E_t}=\left(\frac{\sigma_{cr}}{\sigma_1}\right)\left(\frac{\sigma_1}{E}\right)\left(1+\frac{17(1-0.979)}{0.979}\left(\frac{\sigma_{cr}}{\sigma_1}\right)^{16}\right)$$
$$=s\left(\frac{\sigma_1}{7258.77}\right)\left(1+\frac{17(1-0.979)}{0.979}s^{16}\right)=0.00529s\left(1+0.3647s^{16}\right) \quad (3)$$

$$G=\left(1+\frac{h}{2R}\right)\cdot F \quad (4)$$

$$F=\left(\frac{1}{3\{1+0.4057(L/R)^2\}^2}+\left(\frac{h}{R}\right)^2\left(0.281+\frac{0.624}{1+0.4057(L/R)^2}\right)\right) \quad (5)$$

Where, F and G are parameters determined by the dimension of the pressure vessel and another parameter S is σ_{cr}/σ_1. R and h are mean radius and thickness of pressure vessel. E_t is the tangential modulus and σ_{cr} is the collapse stress, respectively.

In this study, the dimensions which are convenient for users was obtained by computing the variation of the collapse pressure due to buckling for the thickness of the inner space of the pressure vessels such as L=500~700mm, D_i=250~350 mm, t=20~30mm.

Firstly, the authors computed the collapse pressures, changing the thickness (t) and the inner radius (R_i) in a situation where the length (L) of the cylinder is fixed (see left of Fig. 10). Secondly, the authors also observed the variation of the collapse pressures, changing the thickness (t) and the length (L) of cylinder in a situation where the inner radius (R_i) is fixed (see right of Fig. 10).

Investigating the computation results of the collapse

pressure as shown in Fig. 10, it was found that the collapse pressure became larger as the diameter and the length become smaller, and it varied linearly for the thickness. The variation of the collapse pressure of cylinder is influenced much more by the variation of the diameter than that of the length.

As a consequence, the designed cylindrical part of the pressure vessel has been calculated by formulae (3), (4), (5) and S-G graph, and the collapse pressure is about 711bar, so it is estimated to be safe until a depth of 7,110m.

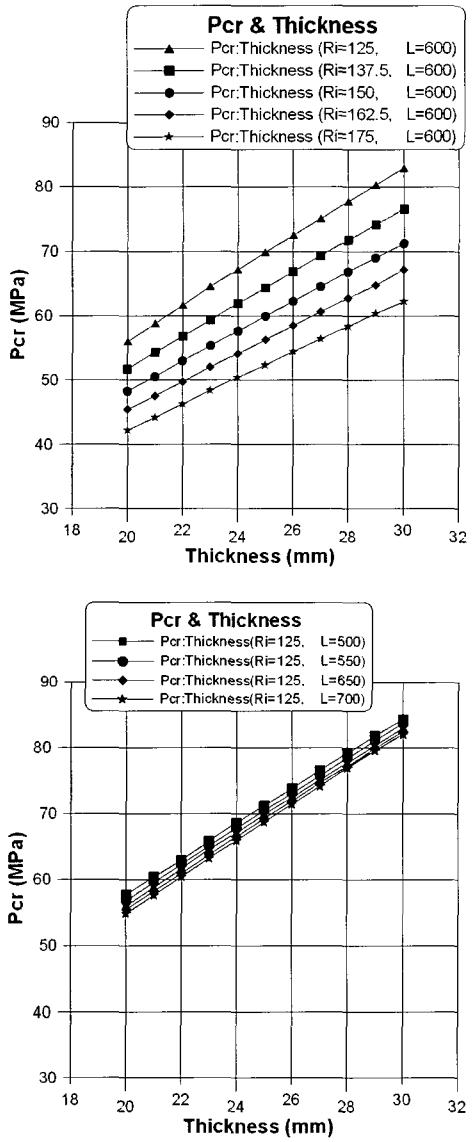

Fig. 10 Collapse pressure of the stiffened cylinders

4.2.2 The stiffened cylinder

The collapse pressure due to buckling of the stiffened cylinder is computed using the formulae based on ABS rules. The buckling behavior is investigated by classifying into the inter-stiffener buckling and overall buckling behaviors (ABS, 1990).

a. Overall buckling strength

The collapse pressure (P_n) due to overall buckling is as following (ABS, 1990):

$$P_n = \left(\frac{Et}{R}\right)A_1 + \frac{EIA_2}{LR^3} \tag{6}$$

Where, E is elastic modulus, I is moment of inertia of combined section including the stiffener, t is the shell thickness, R is the radius, L is the total length of the pressure vessel, and parameters A_1 and A_2 are described as follows (ABS, 1990):

$$A_1 = \frac{\lambda^4}{(A_2 + (\lambda^2/2))(n^2+\lambda^2)^2}, \quad A_2 = (n^2) - 1 \tag{7}$$

Where, λ is $\pi R/L_c$, L_c is the effective length between stiffeners, and n is the lobe number which is taken when the collapse pressure is smallest among integral numbers over 2 being used. The maximum allowable working pressure is calculated through multiplying the parameter considering safety parameter η (0.50) to the computed value P_n. The pressure for the overall buckling mode ofthe designed cylinder is 1,031 bar, which seems to be safe from overall buckling mode, up to a maximum depth of 10,310m under sea level.

b. Inter-stiffener strength

Inter-stiffener strength (P_c) can be determined as follows (ABS, 1990):

$$\begin{aligned} P_c &= P_m/2 && \text{if } P_m/P_y \le 1 \\ P_c &= P_y[1 - P_y/(2P_m)] && \text{if } 1 \le P_m/P_y \le 3 \\ P_c &= (5/6)P_y && \text{if } P_m/P_y > 3 \end{aligned} \tag{8}$$

where,

$$P_m = \frac{2.42E(t/(2R))^{5/2}}{(1-\nu^2)^{3/4}[L/(2R) - 0.45(t/(2R))^{1/2}]}, \quad P_y = \frac{\sigma_y \cdot t/R}{1-F},$$

$$F = \frac{A(1-(\nu/2))G}{A + t_w t + (2NtL/\theta)}, \quad A = A_s(R/R_s)^2,$$

$$N = \frac{Cosh(2Q) - Cos(2Q)}{Sinh(2Q) - Sin(2Q)}, \quad Q = \theta/2, \quad M = L\sqrt{Rt}.$$

The maximum allowable working pressure is calculated through derived inter-stiffener strength (P_c) multiplied by the parameter η (0.50) (ABS, 1990). The calculated result for the

designed pressure vessel shows that the maximum allowable pressure is 650bar, and it seems to be safe from inter-stiffener buckling up to 6,500m under sea level.

5. Conclusions

5.1 Structural design and analysis of launcher and ROV frame

In this study, the structural analysis for the basic frames of the 6,000 m class ROV and launcher was conducted and the structural safeties of them were examined.

5.1.1 The Launcher

In the case of the launcher frame, through the process of optimization for the various sections, the weight was reduced by 116kg (42%), within the range of constraints satisfying a standard safety factor of 8.

5.1.2 The ROV

In the frame of the optimized ROV, the maximum stress level is about 61MPa, which was decreased by 5MPa (7.5%) compared with that of initial design. And the weight of it becomes 245kg, which is about 86kg (about 26%) lighter than that of initial design. The safety factor of the maximum stress for optimum design is about 4.5. This would be insufficient considering the design standard safety factor of 8. But the distribution of overall stress level except the joint of the lift ring is 27MPa, which means the safety factor is over 10. Therefore, if the joint for lifting is properly reinforced, it is considered that the overall structural system will be safe.

5.2 Structural design and analysis of the pressure vessels

Safety for the cylindrical pressure vessel have been examined by analyzing two cases, the ring stiffened cylinder and the unstiffened one. In the linear-elastic analysis, it is shown that FEA results using the 2-D axi-symmetric element have a high degree of agreement with the analytical results. The stress level of designed pressure vessels shows lower than yielding stress.

The design check was carried out by analyzing two cases considering the overall buckling and the inter-stiffener buckling.

5.2.1 The unstiffened cylinder

The results of linear-elastic analysis show that the designed pressure vessel is safe until a depth of 8,279m.

According to buckling collapse pressure formulae, it seems to be safe until a depth of 7,110m. Therefore, it was known that the collapse of the cylindrical part of pressure vessel is dominated by buckling.

5.2.2 The stiffened cylinder

The linear-elastic FE analysis results for the stiffened cylindrical part of the pressure vessel compared with those for the unstiffened cylinder showed that the maximum stress of the stiffened cylinder part of the pressure vessel occurred in the inner surface of the wall, was about 10MPa higher than those of the unstiffened cylinder part. The overall stress distribution level, however, was reduced by 20~80MPa and the total weight was reduced by approximately 4kg compared with that of the unstiffened cylinder.

The results of the linear-elastic analysis show that the initially designed stiffened cylinder seems to be safe until a deep-sea depth of 7,100m. According to an allowable working pressure formula based on ABS, initially designed stiffened cylinder is expected to be safe up to the maximum depth of 10,310m against overall buckling and 6,500m against inter-stiffener buckling.

The dimensions of currently designed sections are all satisfying the structural safety criteria.

Aknowledgements

This research is part of results of the development of an advanced deep-sea unmanned underwater vehicle, which is progressing at KORID-MOERI (Korea Ocean Research & Development Institute-Maritime & Ocean Engineering Research Institute), and is funded by the Korean Government (MOEHRD) in 2005 through a grant administered by the Korean Research Foundation (KRF-2005-214-D00221). The authors would thank to Mr. Andy Bowen of WHOI (Woods Hole Oceanographic Institution) and Dr. Taro Aoki of JAMSTEC (Japan Agency for Marine-Earth Science and Technology) for their technical supports and Dr. Karl Sammut of the Flinders University of South Australia in Adelaide.

References

American Bureau of Shipping (1990). "Underwater vehicles, systems and hyperbaric facilities," ABS - Rules for Building and Classing, pp 5-1 - 6-22.

ANSYS (d1994). "Verification manual 5.4," ANSYS Inc., pp 25.1-25.4.

Deepsea Power & Light (2001). "Under pressure 4.01

manual," Deepsea Power & Light Co., pp E-4 - 6.

JAMSTEC (1991). "Design criteria for 10,000m class deep sea pressure vessel," Report of JAMSTEC (Japan Agency for Marine-Earth Science and Technology).

Joung, T.H., Lee, J.H. and Noh, I.S. (2004). "Pressure vessel design and structural analysis of unmanned underwater vehicle," J. of the Society of Naval Architects of Korea, Vol 41, No 6, pp 140-146.

Lee, J.H., Huh, Y.J. and Joung, T.H. (2004). "Optimal design of the deep-sea unmanned vehicle frame using design sensitivity," J. of the Society of Naval Architects of Korea, Vol 4, pp 28-34.

Noh, I.S. and Joung, T.H. (2003). "Structural analysis of pressure vessels for advanced deep-sea unmanned underwater vehicle," KORDI Report UCM0059A-04028, pp 157-229.

O-shima (1971). "Strength of stiffened cylinder with a external high pressure," J. of the Society of Naval Architects of Japan, Vol 490, pp 170-174.

Shin, J.R. and Woo, J.S. (1999). "Collapse analysis for deep sea pressure vessel," J. of Ocean Engineering and Technology, Vol 13, No 4, pp 82-97.

Tae Sung S&E Inc. (2002). "ANSYS training manual design optimization," Tae Sung S&E Inc., pp 259-276.

Ura, T. and Takagawa, S. (1997). Underwater Robot, Naruyamadou, Tokyo, pp 114-120.

Woods Hole Oceanographic Institution (WHOI) Marine Operations Web Home Page (2005). http://www.whoi.edu/marops/vehicles/jason.

Young, W.C. (1989). Roark's formulas for stress and strain, McGraw-Hill Book Co., pp 638-639.

2006년 4월 10일 원고 접수
2006년 5월 25일 최종 수정본 채택